



OPEN

Analysis of voltage rise phenomena in electrical power network with high concentration of renewable distributed generations

Ayodeji Stephen Akinyemi[✉], Kabeya Musasa & Innocent E. Davidson

The increasing penetration levels of renewable distributed generation (RDG) into a power system have proven to bring both positive and negative impacts. The occurrence of under voltage at the far end of a conventional electrical distribution network (DN) may not raise concern anymore with RDGs integration into a power system. However, a penetration of RDGs into power system may cause problems such as voltage rise or over-voltage and reverse power flows at the Point of Common Coupling (PCC) between RDG and DN. This research paper presents the impact of voltage rise effect and reverse power flow constraint in power system with high concentration of RDG. The analysis is conducted on a sample DN, i.e., IEEE 13-bus test system, with RDG penetration by considering the most critical scenario such as low power demand in DN and a peak power injection by RDG. For studying the impact of voltage rise and reverse power flow, a mathematical model of a DN integrating RDG is developed. Furthermore, a controller incorporating an advance control-algorithm is proposed to be installed at PCC between DN and RDG to regulate the voltage rise effects and to mitigate the reverse power flow when operating at a worst critical scenario of minimum load and maximum generation from RDG. The proposed control strategy also mitigates the voltage-current harmonic distortions, improves the power factor, and maintain the voltage stability at PCC. The simulations are carried out using MATLAB/Simulink software. Finally, recommendations are provided for the power producers to counteract the effects of voltage rise at PCC. The study has demonstrated that, voltage at PCC can be sustained with a high concentration of RDG during a worst-case scenario without a reverse power flow and voltage rise beyond grid code limits.

List of symbols

\hat{V}_a	Sending end voltage
\hat{V}_b	Receiving end voltage
R	Resistance of the line
X	Reactance of the line
\hat{I}	Current flows through the line
P	Real power flowing through the network to the load
Q	Reactive power flowing through the network to the load
P_{Load}	Real power of the load
Q_{Load}	Reactive power of the load
P_{RDG}	Renewable distributed generation active power
Q_{RDG}	Renewable distributed generation reactive power
P_L	Active power of the load
Q_L	Reactive power of the load
$R + jX$	Impedance of the line
(\hat{f})	Amplitude of the line to neutral

Department of Electrical Power Engineering, Faculty of Engineering and the Built Environment, Durban University of Technology, Durban 4000, South Africa. ✉email: 21960204@dut4life.ac.za

w_0	AC frequency
θ_0	Phase angle
(V_{null})	Voltage of the AC system neutral point
(V_{sq})	Voltage output
(I_d) and (I_q)	Control input
(I_{id}) and (I_{iq})	Disturbance inputs
V	Positive voltage sequence
Vref	Reference voltage
Xs	Slope/droop resistance
I	Reactive current
I > 0	Inductive current

The integration of RDG into the power system is ever increasing on daily basis which can be ascribable to the policy regulation of energy because of global warming, increasing environmental concerns of the adverse effect of fossil fuel usage, regular outage and blackout, inadequate access to the utility grid by the rural communities and the high price of electricity billing^{1–3}. The conventional power system has been intrinsically radial, i.e., power flows in one direction only: from power plant to transmission network, distribution network, and to the loads. These flows are traditionally managed through the dispatch of generation and network equipment such as tap-changing transformers that can adjust network voltages, i.e., the voltage settings at the last controllable transformer before the loads are often set at 5–10% higher than the nominal end-use voltage to accommodate line losses and voltage drops along the line. These losses and associated voltage drop depend, of course, on the actual current flows that are being demanded by the loads. However, the introduction of RDG changes the dynamic of the network because power flows may change significantly and potentially in both directions. In other words, the network becomes an active system with power flows and voltages determined by the mix of centralized power, RDG and as well as the load. Thus, with significant increase in penetration level of a large RDG, over voltage will occur at PCC, the voltage at the load end would be greater than the feeder supply voltage, this is called the voltage rise and can also cause the voltage to flow back to the feeder supply side known as reverse power flow. The reverse power flows and voltage rise are worsened when customer demand is at its lowest and RDG supply is at its highest, such issue would be critical especially on the long feeders such as in rural areas. Repeated switching of RDG systems on and off or complete disconnection of RDG from the grid and other methods suggested in Refs.^{4–14} in response to voltage rise and the reverse power flow issues could only provide a temporary measure. Consequently, the resultant effects can impose consequent cycling of network voltage control equipment with associated asset life and maintenance impacts, can cause partial/total outages or excessive under voltages at the far end of the DN, damaging online power component, end-use equipment and voltage instability^{15–17}. Hence, permanent solution is required.

Similarly, there are several technical issues reported by distribution system operators (DSO) that are associated with the increase in penetration level of RDG integration such as voltage rise, voltage instability during grid disturbance, power flowing back to the substation, voltage-current harmonic signals, etc.¹⁸. These challenges may persist for a long period of time if DSO does not have a foreknowledge of the power flow with RDG integration, which can cause serious damage to the power system components/equipment and the load connected to the system. For RDG penetration level to be sustained without disconnection from the system, an over voltage at PCC must be managed. The power flows and the voltage profiles of a traditional electrical distribution system cannot remain the same when considerable amounts of renewable energy-based distributed generation are integrated. Typical RDGs inject active power into the grid, increase in penetration level may cause an over-voltage/voltage rise at the PCC which must be regulated as specified by IEEE 1547 if the facilities are to continue operation.

The operating condition of DN would be vital when considering a large RDGs with increasing penetration level due to the potential voltage rise and the reverse power flow threat at PCC. The PCC voltage rises at the critical scenario of low load and peak RDG generation, such that the depth of voltage rise depends on the injection of active and the reactive power from the RDG. The bidirectional flow of energy from the RDG as well as the main utility grid causes several difficulties regarding the DN voltage profile, power quality, security, power flow control, energy management, frequency control and protection. Network protection and security when a large RDG is connected to DN has been a significant concern in recent years and needs an urgent attention. The RDG injects active and the reactive power to the grid at the PCC. Thus, PCC point is more active than other nodes in the system, often the PCC's voltage is higher than other Busbar voltages within the network. The more the PCC is becoming an active point due to the increase in the RDG penetration level, there would be a voltage rise and the reverse power flow threat at the PCC. The voltage rise beyond the required limit set by the utility will occur at the critical scenario. At this critical stage, it is either RDG is disconnected from the network to avoid damage to other facilities within the system or the voltage rise and the reverse power flow occurrence are regulated to an acceptable range. The unprecedented behaviour of the feeder due to the impact of a large RDG system has drawn keen interest of researchers worldwide and it has resulted in the development of analytical tools for investigating these impacts to develop mitigation measures to curb some of the issues and challenges on distribution feeders.

A considerable number of research efforts have been carried out in the literature to assess the impact of voltage rise with RDG integration and to provide grid support among different voltage controls. In most of the foregoing literature, the researchers have only focused on generation curtailment in DN with RDG integration. Nevertheless, a few studies have been explored to alleviate voltage violation. Reference¹⁹ established that voltage rise depends on the value of line resistance and real power injection. With the advent of over generation of power from RDG, there may be a need to curtail some RDG real power or absorb reactive power by RDG inverters to eliminate the voltage rise. It is also established that highest voltage rise may occur at the farthest bus

after the RDG integration in the DN. It is also observed in Ref.²⁰ that with an increase in the RDG penetration level to DN, the voltage rise increases, and this increase in the voltage rise is attributed to the impedance of the line. Reference²¹ proposed phase shifting strategy (PSS) for mitigation of the voltage rises and reverse power flow. On-Line-Tap-Changer (OLTC) in conjunction with D-STATCOM were used to mitigate the voltage rise in DN^{22,23} while²⁴ proposed two D-STATCOM and OLTC for voltage regulation and to mitigate voltage unbalance in DN. Reference²⁵ utilized dynamic voltage restorer (DVR) that utilizes a matrix converter to mitigate power quality problems such as voltage dip, swell and obtained the compensation energy directly from the power system. References^{26,27} established that there would be a reverse directionality of the power flow to the electric grid with RDG integration and low load consumption. The reverse power flow constraint at PCC caused by a high concentration of RDGs and a minimum power demand in DN were also buttressed in the literature review with mathematical analysis; and it has been demonstrated that, increasing of power output from RDGs will inevitably cause a rising of voltage at PCC. This voltage rise may spread throughout the feeder/or source in case more RDGs are connected to the main knot of the feeder. It is also suggested in Ref.²⁸ that the mitigation of voltage rise can be achieved by controlling the active and reactive powers using a voltage source converter.

The performance of the voltage rise during transient faults when RDG sources are integrated to DN has been consistently investigated. The ability of RDGs to stay connected to the grid during fault conditions for a specified period is referred to as low voltage ride-through (LVRT) ability in the literature reviewed^{29,30}. Various advanced techniques have been provided by the researchers to improve the RDG ride-through capability where most of the control strategies adopted techniques worked in normal operation mode and under a fault condition³¹. The response of a RDG to a short circuit fault depends on the type of renewable generators employed as described in Refs.^{32,33}, if a fault is applied at the terminal of a RDG, the short circuit current can reach up to five to six per unit (p.u.) of the rated voltage/current that could damage the generator. Reference³⁴ recommended an approach to enhance the low voltage ride-through ability based on inductance-simulating control to coordinate voltage/current which minimized the post-fault current within the acceptable range. Reference³⁵ suggested an improved fault ride-through for a RDG under symmetrical and unsymmetrical faults, the scheme trusted with the control of the inverter and grid side converters to decrease overcurrent and inject reactive power to the grid side to support voltage recovery. References^{36,37} developed an optimum resistive type of fault current limiter to achieve maximum fault ride-through capability with RDG which is an effective control strategy for a low voltage ride through for RDG. In addition, increase in the penetration level of the RDG to the DN can cause transient overvoltage during rapid earth fault which may lead to wildfire. It may also trigger some sensitive overvoltage protective devices. The effects could be mitigated by the voltage clamping-based overvoltage protection strategy that has proposed and developed through a smart power electronic topology³⁸. Moreover, the previous studies have not conducted a comprehensive analysis of voltage rise effects and reverse power flow with RDG integration at the PCC of a DN in alleviating voltage rise concerns. However, due to the rising number of RDG installations in the DN, new voltage management approaches are required to be adopted to mitigate the voltage rise concerns. This paper presents the analysis of voltage rise effects with RDG integration at the PCC of a DN. The following are the research questions that guide the study:

- Can high concentration of RDGs integration cause a voltage rise on a distribution network?
- What effect or impact will the RDGs have on the reverse power flow into a distribution network?

If there is adequate information and understanding of how RDG integration and penetration level will appear in a distribution network as this will expand the monitoring efforts of DSO to operate the grid efficiently and economically in reaction to the evolving challenges of RDG penetrations into a DN. The contribution of this research paper is as follows:

- This study develops a mathematical model of an electrical distribution network with an RDG—connected. The developed model is further used to investigate the effect of voltage rise on an electrical distribution network.
- To design an advance controller with PWM control-algorithm to normalize the voltage rise at PCC and to mitigate the reverse power flow when operating at a worst critical scenario of minimum power demand and maximum power output from RDG.
- The installation of PWM based DSTATCOM at PCC for the control of active and reactive power.

The solutions developed in this research paper can be useful for DSOs and independent power producers at the planning and installation stage of RDG integration. The paper is structured in three sections. The first section is the introduction while the second section discusses the methods which comprises of the power system design and RDG, Mathematical model derivation for the analysis of voltage rise effects and the description of the test system under investigation. The last section presents the results and discussion which is divided into subheadings, such as the simulation results, voltage rise concept, the impact of RDG on a distribution network, RDG integration versus voltage rise at PCC, the voltage rise compensation methods, RDG integration and voltage rise at PCC, voltage rise compensation methods, compensator connection model, signal analysis, small signal analysis and voltage rise regulation, simulation analysis are presented while eight summarizes the conclusion.

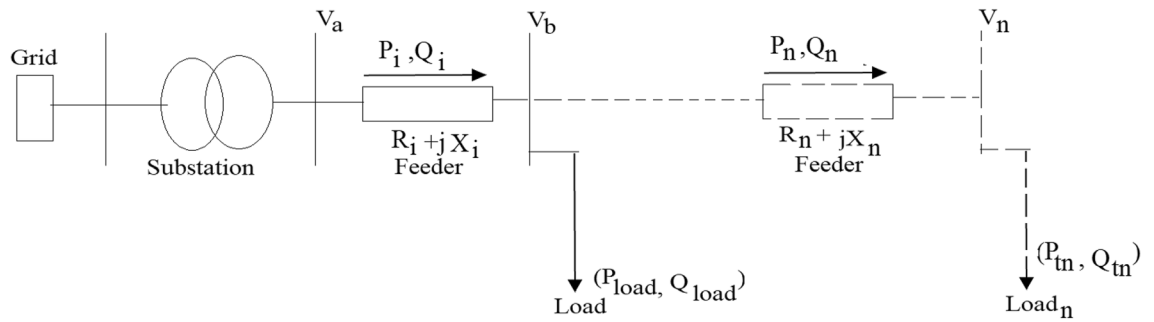


Figure 1. Equivalent circuit of an electrical distribution system.

Comparison between conventional power system and RDG design		
S/N	Conventional	RDG
1	Unidirectional power flow	Bidirectional power flow
2	Centralized generation	Distributed generation
3	Manual monitoring	Self-monitoring
4	Manual restoration	Automatic restoration
5	One-way communications	Two-way communications
6	Electromechanical	Digital
7	Few sensors	More sensors
8	Limited control	Full control
9	Failures and blackouts	Adaptive and resilient

Table 1. Power system design and RDG.

Methods

Power system design and renewable distributed generation. In the traditional or conventional electrical distribution networks, generally power flows from the substations to the loads in a unidirectional manner as shown in Fig. 1. Integration of RDGs into the power system has changed the features of the power system; actually, power flows change from unidirectional to bidirectional. Table 1 provides a summary of changes in power system with RDG integration. The active and the reactive power usually flow from higher voltage potential to the lower voltage level, the ratio of reactance to the resistance of the distribution network is also less than or equal to (1/2), while that of the transmission network is greater than or equal 10. Consequently, the value of the resistances in the transmission network is lower as compared to the distribution network, this high resistance in the distribution network is responsible for the voltage drop along the feeders from the sending end to the receiving loads.

Mathematical model derivation for voltage rise analysis. Considering an electrical distribution network in Fig. 1 to analyze the voltage limit violation challenges. This feeder comprised of n buses, and on each bus, loads are connected. The voltage differential between two consecutive buses depends on the line segment impedance and the active and reactive power flows as deduced in Eq. (1). Where V_a and V_b is the sending end terminal voltage and the receiving end terminal voltage as indicated in the Abbreviation section.

$$V_{b-a} - V_b \cong \frac{R_i P_i + jX_i Q_i}{V_b \cong 1p.u.}, \tag{1}$$

where P_i and Q_i are the active and reactive power flow through the i_{th} section of the line which depend on the active and reactive power absorbed in the feeder buses. When power losses are neglected, Eqs. (2) and (3) can be deduced.

$$P_b \cong P_{b-a} - P_{t_{b-a}}, \tag{2}$$

$$Q_b \cong Q_{b-a} - Q_{t_{b-a}}, \tag{3}$$

where P_{t_b} and Q_{t_b} are the active and reactive power absorbed in the i_{th} bus, which are equal to the difference between the power consumption of the load (P_{Load} and Q_{Load}) and the output power of the RDG (P_{RDG} and Q_{RDG}) connected to this bus is deduced in Eqs. (3) and (4).

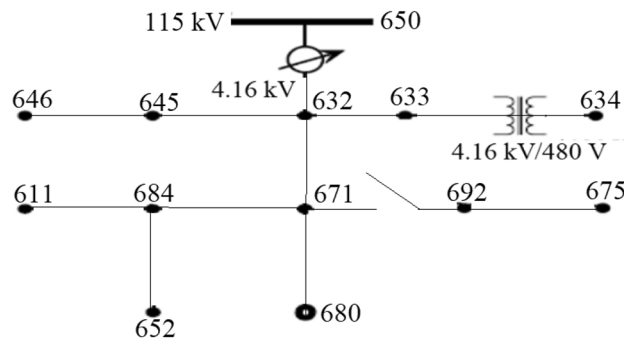


Figure 2. IEEE 13 Node feeder test system.

$$P_{tb} \cong P_{Load} - P_{RDG}, \quad (4)$$

$$Q_{tb} \cong Q_{Load} - Q_{RDG}. \quad (5)$$

From the Eq. (1), the voltage difference between the i_{th} bus and the main substation bus can be expressed in Eq. (6).

$$\begin{aligned} V_{sub} - V_b &= \sum_{j=1}^b R_j P_j + X_j Q_j = \sum_{j=1}^b R_j \left(\sum_{k=j}^n P_{t_k} \right) + X_j \left(\sum_{k=j}^n Q_{t_k} \right) \\ &= R_1 (P_{t_1} + \dots + P_{t_n}) + X_1 (Q_{t_1} + \dots + Q_{t_n}) + \dots + R_b (P_{t_b} + \dots + P_{t_n}) + X_b (Q_{t_b} + \dots + Q_{t_n}). \end{aligned} \quad (6)$$

From Eq. (6), when there is no RDGs, the power absorbed by the load increased, then the internal bus voltage decreased relative to the sending end voltage bus. This can cause a voltage drop across the network end buses from its allowable range under high demand scenario. However, with an increase in the penetration level of RDG in the system, during peak generation hours of RDGs and low demand scenario, the power absorbed on each bus reduces resulting in the reverse power flow through the feeder. In this condition, P_{tb} becomes negative, and the internal bus voltage increases relative to the sending end voltage resulting in voltage rise occurrence. Conversely, depending on the location of power absorption or injection in the network, its impact on the system voltage profile is not the same. It is very clear from Eq. (6) that the active and the reactive power injected at the end buses flow through the larger impedance which can create more substantial consequence on the voltage of these terminals. Change in voltage can be expressed in per-unit or percentage and by considering V_a and S_a as base parameters in Eq. (7).

$$\Delta V \approx RP + XQ, \quad (7)$$

where, P and Q are the per-unit active and reactive power; and R and X are the per-unit values of the line impedance. The voltage variation limit at the PCC on demand or consumer sides is very vital for power quality as specified by IEEE 1547 std. The IEEE standard grid code allows a ± 6 voltage variation at PCC when connecting RDG to an electrical network, while the South Africa grid code regulation allows -15% to $+10\%$ (0.85 to 1.1 voltages per unit) for low voltage and $\pm 10\%$ for medium and high voltage around the nominal value³⁹. The voltage level at the point of load connection can be investigated using the standard IEEE 13 Node feeder test system^{40,41} in Fig. 2.

Test system description. Modified IEEE 13-bus test system, shown in Fig. 2 is used in this research paper to investigate the impacts of RDG integration to an electrical distribution network and also to test the performance of the controller for voltage rise regulation. The IEEE 13-bus test system is a sample standard distribution network for voltage profile analysis. It is comprised of both the medium and the low voltage distribution network interconnected via a three-phase 4.16 kV/480 V transformer. This model was developed by the IEEE Power Engineering Society's Power System Analysis, Computing and Economics Committee^{42,43}. The test system is modified and modelled as balanced three phase in the MATLAB/Simulink environment; all the underground lines are modelled as overhead lines because there is no underground cable in the Simpower system's library of Simulink. The network loading is modified to be 480 kVA to 1 MVA while the capacity of the distribution station is 510 kVA with 4.16 kV voltage level, the total length of the network is 25 km. The detail parameters of the system are depicted in "Appendix".

Results and discussion

Test system simulation. The test system is simulated, the measured bus voltage and the graphical representation of the measured voltage parameters obtained from the system are shown in Table 2 and Fig. 3. The network allowable voltage variations are guided by the IEEE 1547 which allow ± 6 variation in PCC voltage and South Africa grid code that allows -15% to $+10\%$ (0.85 to 1.1 voltages per unit) for low voltage and $\pm 10\%$ for

Bus no	Voltage (pu)
632	0.9498
633	0.9497
634	0.9495
645	0.9495
646	0.9494
671	0.9492
692	0.9490
675	0.9488
684	0.9486
611	0.9484
652	0.9482
680	0.9480

Table 2. Base case measured voltage.

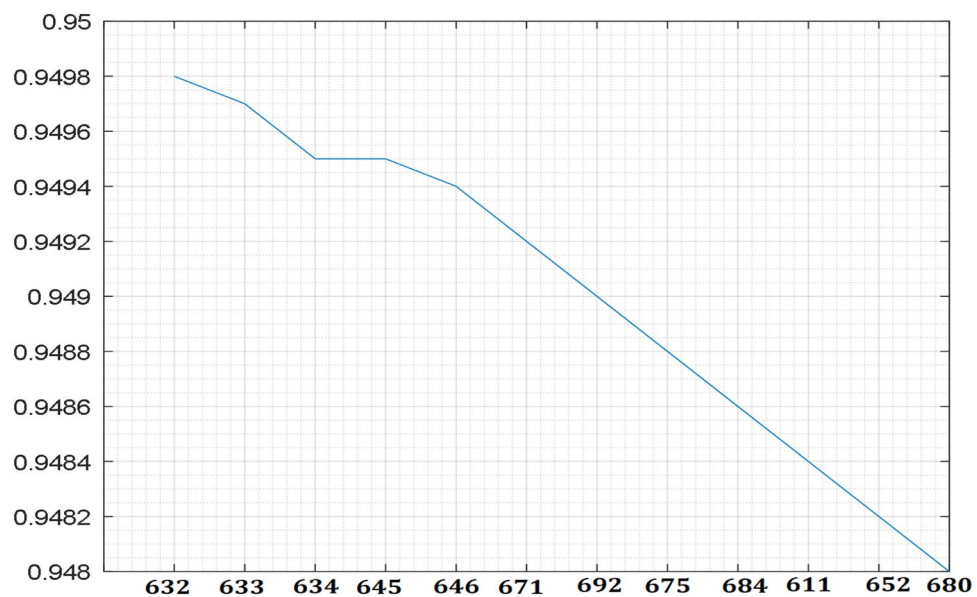


Figure 3. Test system voltage profile.

medium and high voltage around nominal voltage^{39,44}. It is observed that the system voltage profile variations are within the specified limit of both ± 6 and -15% to $+10\%$. However, if the distance of the distribution line in Fig. 1 is assumed to be longer than 25 km and the network loading is greater than the current loading, by analogue thinking, the farthest nodes such as node 652 or 680 of the voltage profile in Fig. 3 will fall outside the specified voltage limit. Hence, utility company usually runs their networks to be within the allowable voltage ranges and regulates the network voltage with the aid of automatic voltage regulator and on tap changing transformers.

Voltage rise concept. The conventional distribution networks usually designed to have a stable voltage profile initially such that the voltage rise may not be the concern² but under voltage, meanwhile, when RDGs are integrated into the network, the power flow is no more unidirectional such that power flows is not only from the substation to the farthest node of the system anymore, but the power can also now flow back from the farthest node towards the substation due to the RDG integration. The system voltage profile would definitely be affected by the RDGs integration because the network is no more passive but has become an active network. The voltage generated by the RDGs must be higher as compared to the voltage of the other nodes around the PCC for the power to be exported to another part of the network. This can be best described by the Eq. (7) and the equation parameters are described in the Abbreviation section. Therefore, the receiving end voltage (V_b) can be expressed in Eq. (8).

$$V_b \approx V_a + RP + XQ. \quad (8)$$

The change in the power flow direction because of RDG integration resulted to the generated voltage at PCC to rise above the sending end voltage such that the node at which RDG is connected to a distribution network

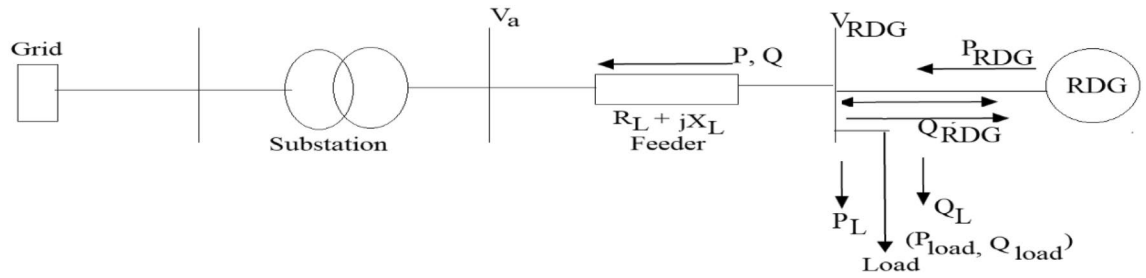


Figure 4. RDG integration to distribution network.

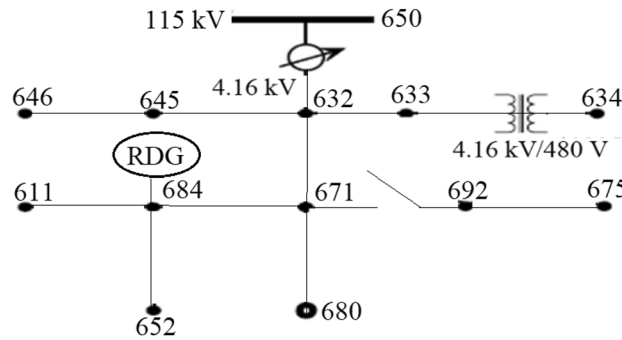


Figure 5. RDG connection to distribution network.

will form active point, the weak node will become an active node, further increase in the number of RDGs and their penetration levels will also make the nodes near the PCC to be more active resulting to fewer weak zones in the system. Hence, active zones become smart zone, further increase in RDGs penetration levels will eventually result in a sufficient smart point to control the whole local network. The more the PCC is becoming active point, there is a potential voltage rise threat at that point if the voltage at that point is not regulated which can be analysed in Fig. 4.

RDG is integrated into a distribution network via the distribution line with impedance as shown in Fig. 4, the nomenclature of the circuit equations is defined in the nomenclature table. The rise in voltage at PCC due to the RDG integration can be expressed in Eq. (9).

$$\Delta V = V_{RDG} - V_a \approx \frac{RP + XQ}{V_{RDG}}, \tag{9}$$

where $P = (P_{RDG} - P_L)$ and $Q = (-Q_L \pm Q_{RDG})$.

From Eq. (9), V_{GEN} can be expressed in term of per unit in Eq. (10).

$$\Delta V = V_{RDG} - V_a \approx R(P_{RDG} - P_L) + X(-Q_L \pm Q_{RDG}). \tag{10}$$

Most of the time, RDG exports active power ($+P_G$) to the grid and the reactive power ($\pm Q_G$) can also be exported or imported from/or to the grid while the load active and the reactive power (P_L and Q_L) are being consumed by the loads. Depending on the type of RDG that is integrated into the distribution network, some export real power to the grid when the loads connected to the system reduce below the generator output, whereas reactive power could be exported or absorbed depending on the settings of excitation scheme of the RDG such as synchronous generator when it is use for wind energy converter while induction generator consumes reactive power to operate. Solar Photovoltaic exports real power to the grid at a predetermined power factor, the flow of power could occur in both directions based on the real and the reactive power loading of the system as compared to the output of the generator and the system losses.

Impact of RDG on distribution network. This section investigates the impact of RDG on a distribution network. A RDG of 240 kW with a unity power factor is integrated into the network of Fig. 2 as shown in Fig. 5 to meet a certain customer load demand while the distribution substation voltage is controlled at 100%. Tables 3 and 4 depict the measured voltage values from each node of the network while Figs. 6 and 7 depict the graphical representation analysis of the simulation results. It is observed that the network voltage profiles improved considerably with the increase in the RDG integration penetration level and is within an acceptable voltage range. It is also observed that the voltage of the node 684 at which the RDG is connected (PCC) is higher than any other voltages of the network as previously said as shown in Figs. 6 and 7, this is because of the injection of active power by the RDG which makes that particular bus voltage (PCC) to be active than any other node, the impacts are noticeable at the PCC and the closest node in both directions around the PCC. The voltage profiles are within

Bus no	Base Voltage	10%	20%	30%	40%
632	0.9498	0.9498	0.9498	0.9498	0.9498
633	0.9497	0.9497	0.9497	0.9497	0.9497
634	0.9495	0.9495	0.9495	0.9495	0.9496
645	0.9495	0.9495	0.9495	0.9496	0.9497
646	0.9494	0.9494	0.9494	0.9495	0.9497
671	0.9492	0.9492	0.9492	0.9493	0.9497
692	0.9490	0.9491	0.9492	0.9493	0.9497
675	0.9488	0.9489	0.9490	0.9492	0.9498
684	0.9486	0.9490	0.9493	0.9496	0.9499
611	0.9484	0.9488	0.9490	0.9493	0.9499
652	0.9482	0.9486	0.9488	0.9490	0.9498
680	0.9480	0.9484	0.9487	0.9489	0.9496

Table 3. Measured voltage at (10–40%) RDG.

Bus no	50%	60%	70%	80%
632	0.9498	0.9598	0.9998	1.0112
633	0.9497	0.9697	0.9997	1.0212
634	0.9496	0.9696	0.9996	1.0221
645	0.9497	0.9697	0.9997	1.0231
646	0.9497	0.9697	0.9997	1.0245
671	0.9497	0.9697	0.9997	1.0368
692	0.9497	0.9697	1.0011	1.0459
675	0.9498	0.9698	1.0101	1.0487
684	0.9499	0.9723	1.0249	1.0593
611	0.9499	0.9700	1.0111	1.0491
652	0.9498	0.9699	0.9999	1.0419
680	0.9496	0.9699	0.9899	1.0391

Table 4. Measured voltage at (50–80%) RDG penetration.

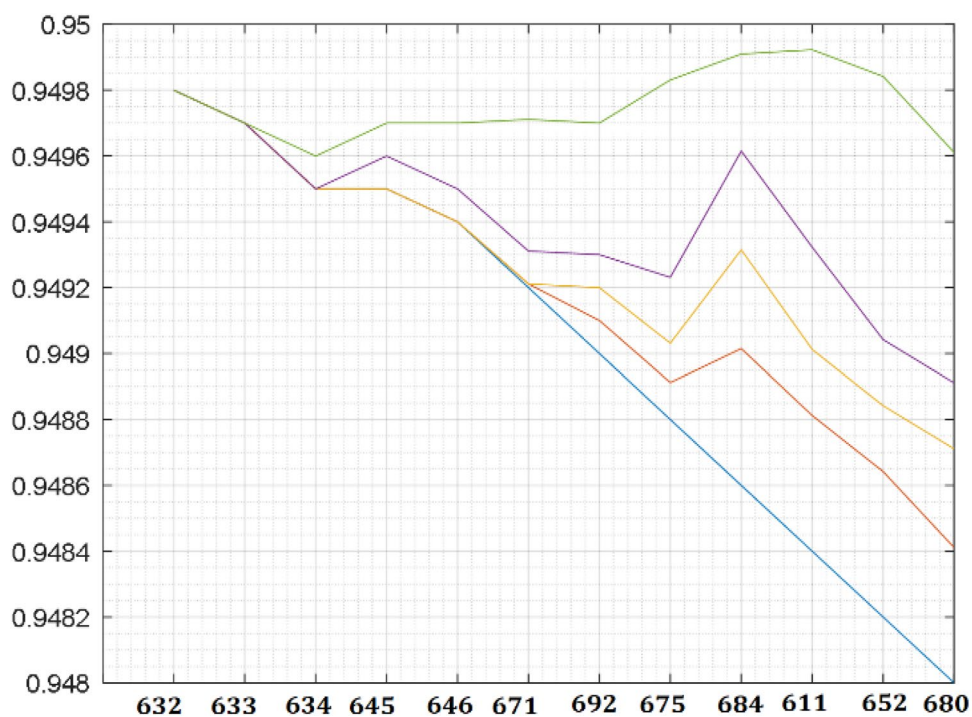


Figure 6. Improved DN voltage profiles at (10–40%).

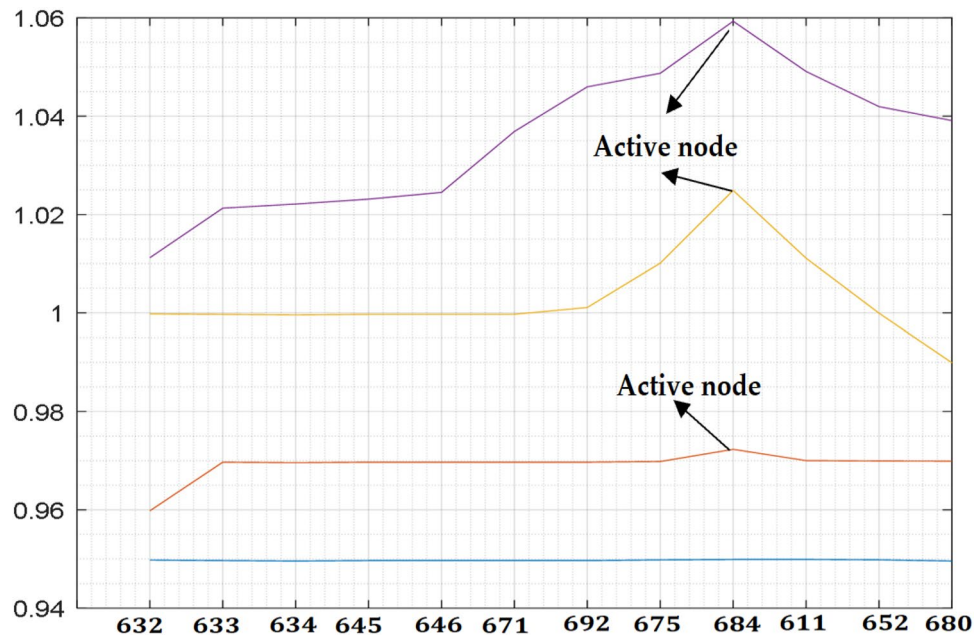


Figure 7. Improved DN voltage profiles at (50–80%).

Bus no	60%	70%	80%	90%	100%
632	0.9598	0.9998	1.0112	1.0420	1.1412
633	0.9697	0.9997	1.0212	1.042	1.1412
634	0.9696	0.9996	1.0221	1.0431	1.1421
645	0.9697	0.9997	1.0231	1.0639	1.1431
646	0.9697	0.9997	1.0245	1.0694	1.1545
671	0.9697	0.9997	1.0368	1.0831	1.1668
692	0.9697	1.0011	1.0459	1.0894	1.1745
675	0.9698	1.0101	1.0487	1.0998	1.1987
684	0.9723	1.0249	1.0593	1.1200	1.2111
611	0.9700	1.0111	1.0491	1.0899	1.1791
652	0.9699	0.9999	1.0419	1.0769	1.1619
680	0.9699	0.9899	1.0391	1.0699	1.1591

Table 5. Measured voltage at 1 MW penetration level.

an acceptable range as specified by IEEE 1547 and the South Africa grid code act of RDG connection at PCC. The investigation of the impacts of RDG integration into power system based on the research investigation and the simulation carries out with the results obtained in this section implies that the impact of RDG integration will improve the distribution network voltage profiles and make the weak node/bus/network active. Hence, a weak node can become an active node with RDG integration while a weak network can become an active network. With the voltage profiles improvement with RDG integration as established in the results (Tables 3, 4, Figs. 6, 7) of the investigation carried out in this paper, the first research question is satisfied such that the impact of RDG with an increase in penetration levels can be noticeable in the power system.

RDG integration and voltage rise at PCC. The network loading remains the same while penetration levels of RDG into the network increases from 240 kW at bus 684 to 1 MW, the buses measured voltages are depicted in Table 5 and the graphical analysis of the simulation are shown in Fig. 8. The increase in the RDG penetration levels causes reverse power flow towards the distribution substation as depicted in Fig. 8 around the nodes 675 and 692. The voltage at bus 684 (PCC) rises above the maximum allowable voltage range of 1.1 pu due to the integration of a large RDG. The over voltage occurs in both directions such that the power flows towards the distribution substation (see Figs. 7, 8, buses 675 and 692) and also to the farthest bus of the network (see Figs. 7, 8, buses 611 and 652). Although, the technical performance of RDG integration can make a weak distribution network to be an active network nevertheless, the impacts of a large RDG can cause voltage rise at PCC and reverse power flows which satisfied the second research question. By analogous thinking, similar occurrence may occur during low load and high generation of RDG integration. It is therefore worthy to note

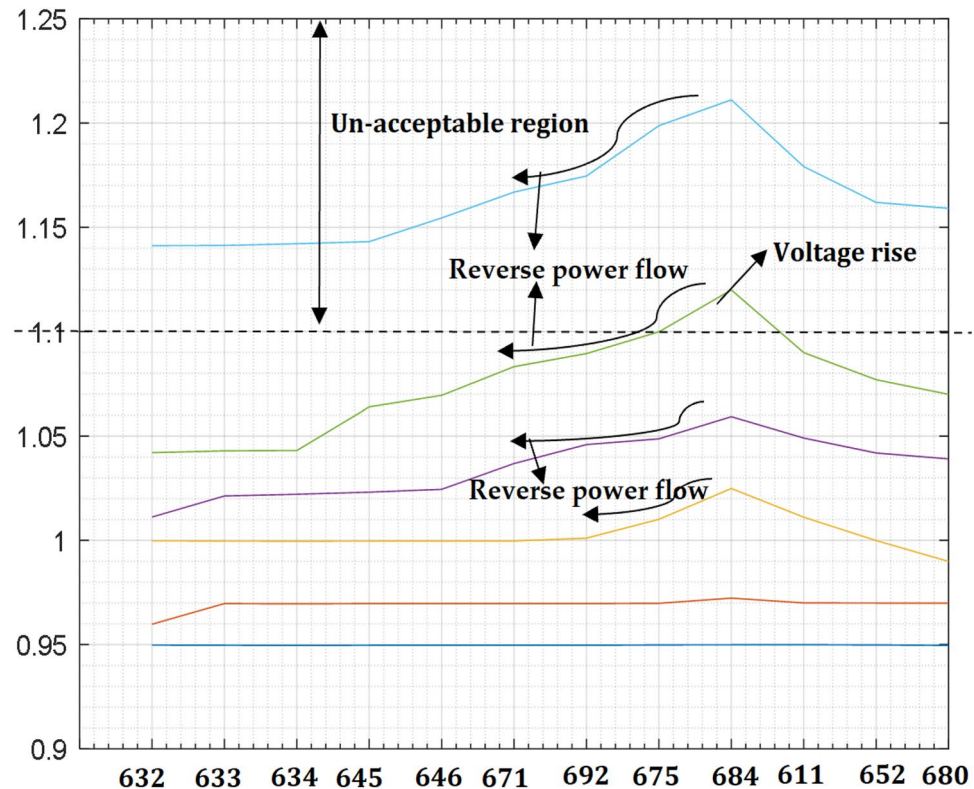


Figure 8. Improved DN voltage profiles at (60–100%).

that before considering RDG for an integration into the power system, the power system operator should consider the possibility of power being exported back to the substation in-case there is an over generation of power from RDG as this will give them the ideal of choice of transformer to be installed that can tolerate the operation of reverse power flow.

The simulation in Fig. 8 satisfies the Eq. (10) such that RDG exports active power ($+P_G$) to the grid. Hence, with RDG integration, the threat that an under-voltage will occur at the far end of the system cannot exist again.

The power system deregulation, reliable power supply, power quality, meeting customers' load demand, economic value and the environmental regulation of greenhouse emissions are some of the primary aims of deploying RGDs integrating into the power system which is seen fulfilling these purposes. Therefore, Eq. (10) can be further expressed in Eq. (11)

$$P_G \approx \frac{P_{RDG} - V_a + RP_L - X(-Q_L \pm Q_{RDG})}{R}. \quad (11)$$

Thus, from the Eq. (11), the level of RDG that can be integrated into a distribution network can be deduced which depend on the following:

- The voltage at the distribution substation.
- The voltage level at the farthest bus.
- The distance of the network and the conductor size.
- Load demand within the network.

There are critical situations that can be investigated and put the outcome into consideration when RDGs are to be integrated into a distribution network to regulate the activities of RDGs at the PCC especially the impacts on the voltage rise such as:

- Peak load and Peak RDG generation.
- Peak load and low RGD generation.
- Low load and Peak RDG generation.
- No load and Peak RDG generation.

If the most critical situation is to be considered such that there is a reduction in the load demanded with a peak RGD generation, the analysis of such situation can be expressed by employing Eq. (10) and re-express in

Eq. (12). Meanwhile, if the network is operating at unity power factor, then the Eq. (13) is valid. Based on this assumption, the Eq. (10) can be re-expressed in Eq. (14).

$$P_L = 0, Q_L = 0, \text{ and } P_{RDG} = P_{RDG \text{ Max}}, \quad (12)$$

$$\pm Q_{RDG} = 0, \quad (13)$$

$$\Delta V_{Critical} = V_{RDG \text{ Max}} - V_a \approx R P_{RDG \text{ Max}}. \quad (14)$$

From the Eq. (14), it can be observed that the PCC voltage rise depends on the resistance (R) of the distribution lines and the penetration power of the RDG. Hence, if the resistance of the distribution line remains unchanged, the Eq. (14) can be re-expressed in Eq. (15), from the Eq. (15), it can be deduced that the amount of voltage in a distribution network with RDGs integration is directly proportional to the active power injected into the network by the RDGs.

$$\Delta V_{Critical} \propto P_{RDG \text{ Max}}. \quad (15)$$

A linear relationship exists between the active power generated by the RDGs and the occurrence of voltage rise at PCC. The voltage rise would be burdensome and raise a concern when there is no load demand in the network due to the fact that the power injected by the RDG would be exported back into the distribution substation and if such thing happens, damaging of power system equipment and components are inevitable. Furthermore, the occurrence of voltage rise at PCC because of impacts of RDGs penetration levels can limit the amount and the extent at which RDG can be integrated into the power system. The above statement can be proved from the Eq. (13), which can be re-expressed in Eq. (16).

$$P_{RDG \text{ Max}} = \frac{V_{RDG \text{ Max}} - V_a}{R}. \quad (16)$$

The amount of RDG that can be integrated into the existing network would be limited by the peak/maximum voltage produced by the RDG connected to PCC which is expressed in Eq. (17).

$$P_{RDG \text{ Max}} \leq \frac{V_{RDG \text{ Max}} - V_a}{R}. \quad (17)$$

Hence, from the critical situation, it can be observed that the resistance of the distribution line and the voltage rise at the network nodes is vital to the amount of RDGs penetration to the distribution network.

Voltage rise compensation methods. With RDG integration into the distribution network, the voltage level of the system will be altered, and power flows will now be bidirectional. With the integration of RDGs into the power system, the voltage sag may not be the foremost concern anymore since active power injected by the RDG will cause the system voltage to increase. Hence, RDG integration introduces a new challenge, the voltage at the Point of Common Coupling (PCC) of RDG is higher as compared to the other buses of the network. Hence, active power increases with an increased penetration level. This results in the voltage increase at the PCC, thereby causes a voltage rise. Voltage rise challenges were reported as the foremost concern against the connection of RDG to medium and low-voltage distribution networks^{45–48}. A large RDGs integration into a distribution network can cause an extreme voltage rise at PCC if not regulated or control appropriately. Conventionally, most of the distribution substations are fortified with an automatic over-voltage protection strategy to safeguard the power system equipment, component and loads of excessive voltage rise⁴⁹. Nevertheless, sometimes the protection scheme arrangement can disconnect RDG permanently from the network or can also disconnect distribution supply from the main grid which can have a critical effect on the customer loads connected to the system and independent power producers causing loss of revenue. The voltage rises at the PCC with RDG integration can therefore be regulated through the following strategies which can be applied at the planning and execution stage of RDG integration by the utility or independent power producers in the power system.

- Reduction in the distribution resistance.
- Distribution substation Voltage control method.
- RDG penetration curtailment.
- Reactive power compensation strategy.

Distribution line resistance reduction. The voltage rise at the PCC poses a great limitation of a large RDG integration into a distribution network. Since voltage is directly proportional to the current flowing through a resistance (Ohm's law), which means voltage increases as current or resistance increases. For alternating current network, the impedance comprises of inductance, resistance and capacitance, by adjustment of these components, voltage increases or decreases. Thus, the voltage drops as a result of the impedance of the feeder, the flow of the current, the load, the transformer and the source voltage define the voltage at the end of the feeder. If the amount of RDG integration into the Distribution network is remained unchanged, thus, Eq. (18) can be deduced from Eq. (16).

$$\Delta V_{Critical} \propto R. \quad (18)$$

The Eq. (18) shows the critical situation whereby the voltage rise from RGD peak penetration is directly proportional to the distribution line resistance. Hence, by reducing the line resistance the voltage rise would be reduced considerably. This process can be logically carried out by increasing the size of the conductors of the distribution network. This method may be slightly difficult to implement on the existing distribution system, but it can be proposed and implemented in the new distribution network. It is therefore recommended for the utility company to put into consideration the reduction in the distribution line resistance by the increasing the conductor size while constructing a new distribution system as this will enable a large RDGs integration to the system.

Distribution substation voltage control method. In a conventional distribution system, it is usually a standard to sustain distribution substation voltage above nominal voltage value. This process is carried out to keep the network voltage within an acceptable range as specified by the IEEE 1547 and South Africa connection act (± 6 or 0.85 to 1.1 pu). However, this situation is not valid when RDGs are integrated into the system as investigated and confirmed in the simulation result in Fig. 8. From the Eq. (19), if the voltage supply from the distribution substation can be controlled, then the voltage drop can be regulated.

$$\Delta V_{Critical} = V_{RDG Max} - V_a. \quad (19)$$

This method of controlling the voltage supply from the distribution substation can easily be carried out using Online Tap Changing Transformer (OLTCT). The voltage regulation is possible in this regard in a short distribution network however, such practice may be cumbersome in a long-distance distribution network because there exist more transformers in a long distribution system, carry out such a practice may not be practicable. Nevertheless, by optimising the supply voltage value and online tap changing transformer tap position, the system voltage can be regulated to the minimum.

RDG penetration level curtailment. The occurrence of the voltage rises at the PCC because of the integration of large RDGs into a distribution can be regulated through the RDGs integration penetration levels curtailment. The consequence of RDGs curtailment can be expressed in Eq. (20), this equation can be re-expressed in Eq. (21).

$$P_{RDG Max} \approx P_{RDG Curtailment} + \frac{V_{RDG Max} - V_a}{R}, \quad (20)$$

$$\Delta V_{Critical} \approx R P_{RDG Max} - R P_{RDG Curtailment}. \quad (21)$$

From the Eq. (21), it can be observed that by curtailing the RDG integration penetration levels, voltage rise can be therefore regulated at PCC. The critical situation is not always occurred such that the minimum load versus the peak RDG generation, therefore, it is desirable to tolerate large RDG integration at PCC and curtail it whenever there is voltage rise occurrence to certain set voltage range. The total amount of RDG curtailment annually can be determined by the no of occurrence of minimum load versus peak RDG generation. The only disadvantage of RDG curtailment is the reduction in the revenue which can affect the utility and the independent power producers because the electricity price is normally being influenced by the amount of load demanded. Logically, the loss of revenue would not be so much as the RDG curtailment will normally occur during the low load and RGD peak generation situation. Hence, the amount of curtail may be moderately low.

Reactive power compensation strategy. Reactive power control is critical in the electrical grid to avoid voltage breakdown, voltage instability, and voltage rise when there is an unusual occurrence or eventualities at PCC. Voltage rise and instability occur in a system wherever there is insufficient of reactive power during RDG over generation, heavy loading and disturbances such as grid faults⁵⁰. Installing Flexible Alternating Current Transmission System (FACTS) devices such as pulse width modulation distribution static compensator (PWMSTATCOM) connected to the PCC of a large renewable farm, dynamic compensation of reactive power and voltage rise control capability can be realized since the lesser the voltage at PCC, the more the reactive power needed⁵¹. It is also very valuable in power system interruptions. Reactive power may be supplied by mechanisms embedded in the network itself and by additional elements inserted into the network to balance the reactive power of this system⁵²⁻⁵⁴. The FACT compensation method should be a requirement for a system with non-linear loads and a large RDGs integration to provide voltage support, attenuate voltage rise at PCC and stability in the event of network disturbance. If the voltage rise at PCC with a large RDGs integration is to be regulated, a compensator device should be installed at PCC⁵⁵ which can be expressed from Eq. (10) to produce Eq. (22). The Eq. (22) can be re-expressed in Eq. (23) and the equation parameters are described in Abbreviation section.

$$\Delta V = V_{RDG} - V_a \approx R(P_{RDG} - P_L) + X(\pm Q_c - Q_L \pm Q_{RDG}), \quad (22)$$

where $\pm Q_c$ = Compensator reactive power (it can generate or absorb reactive power). The voltage rise can be easily controlled with reactive compensator. When the device is strategically installed at the PCC to generate or absorb reactive power, the voltage rise at that point would be considerate minimized, this could also allow more RDG penetration levels without the fear of PCC over voltage or voltage rise.

$$\Delta V = V_{RDG} - V_a \approx R(P_{RDG} - P_L) + X Q_{Import}, \quad (23)$$

where $Q_{Import} = \pm Q_c - Q_L \pm Q_{RDG}$.

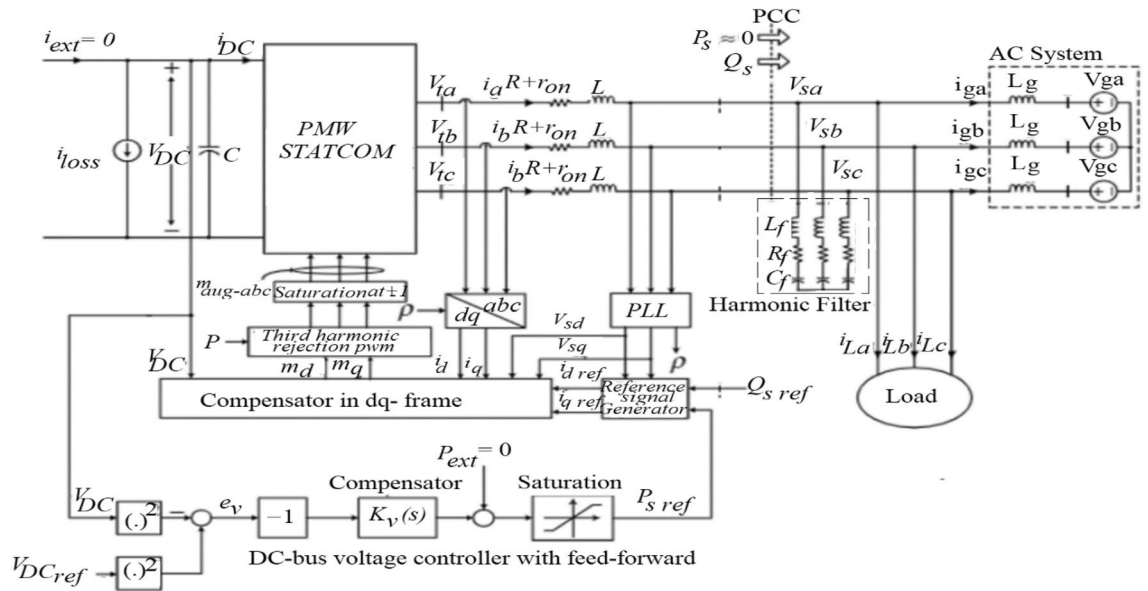


Figure 9. PWMSTATCOM connection to PCC.

If a critical situation is to be considered and the network operates at unity power factor, the Eq. (23) can be re-expressed in Eq. (24).

$$\Delta V_{Critical} \approx RP_{RDG Max} + XQ_{Import}. \tag{24}$$

RDGs always export active power (+ P_{RDG}). Thus, it may also export or import reactive power ($\pm Q_{RDG}$) depend on the RDG parameters e.g., synchronous generator can import power at a 0.96 power factor, whereas a wind turbine with uncompensated induction generator can import power at about a 0.9 power factor. Whereas the load consumes both active (P_L) and reactive (Q_L) power. The compensators may export or absorb reactive power ($\pm Q_c$) depend on the voltage rise occurrence at PCC. From the Eq. (24), it can be deduced that the increase in the amount of reactive power imported would bring the regulation of voltage rise at PCC. The higher the negative value of (XQ_{Import}), the lower the reduction in the voltage rise at PCC, this statement would be verified in the simulation carried out in the next section.

Compensator modelling. System compensation is carried out in this section to mitigate the voltage rise at the PCC with a large RDG integration to a distribution network. The pulse width modulation distribution static compensator (PWMSTATCOM) is connected to the test system in Fig. 5 at PCC to mitigate the voltage rise by generation/absorption of reactive power to the system. PWMSTATCOM parameters are grouped in two categories: Power and Control tab. Converter rating, current, nominal voltage, DC link voltage, impedance, and capacitance rating are specified in power tab while control tab consists of modes of operation (var and voltage control) and droop that control the slope (the regulator gains K_p and K_i). PWMSTATCOM is a circuit-fed reactive power compensation device which is able to produce and/or absorb reactive power, such that the precise data of the grid is controlled to modify the output voltage⁵⁶. It rectifies the direct current input (DC) voltage in an AC output voltage to complement for the active and reactive power required by the system⁵⁷. The PWMSTATCOM schematic representation and connection model to PCC is depicted in Fig. 9, 3-phase voltage source (V_{ga} , V_{gb} , and V_{gc}) represents an AC system which in series connection with a transmission line, (L_g) represent inductance of the line while the resistance and transformer are assumed to be negligible. By controlling the real power of the system, (V_{dc}) can be regulated. The (V_{dc}) is supported by a direct current source which can be a DC energy source such as battery banks and (P_s) compensates for the device power loss.

The electrical nodes on the PWMSTATCOM connection to the 3-phase AC constitute PCC and the voltage at that point are (V_{sa} , V_{sb} and V_{sc}). The phase lock loop PLL input is taken from PCC, and 3-phase loads are also supplied from the PCC. 3-phase RLC filters are connected in shunt with the PWMSTATCOM at PCC to filter unwanted, current harmonics, amplitude and frequency signals of the load voltage from flowing into the grid. The PWMSTATCOM has constant current characteristics when there is under-voltage/over-voltage, below/above the boundary, which permits PWMSTATCOM to provide constant reactive power^{57,58}. The relationship between the Alternating Current of the network voltage and the voltage at the PWMSTATCOM alternating current side terminals offers the influence of reactive power flow. When the terminal voltage of the PWMSTATCOM contact is above the network voltage, PWMSTATCOM would inject reactive power to the grid and PWMSTATCOM act like a capacitor. As soon as the PWMSTATCOM voltage is below the AC voltage, PWMSTATCOM functions as an inductor and the reactive power flow is reversed, when the network voltage is equal to the PWMSTATCOM voltage, there is no energy exchange^{59,60}. The modelling of PWMSTATCOM's dynamic voltage regulation at PCC involves linearizing the non-linear circuit elements at the operating point of PWMSTATCOM and when the behaviour becomes non-linear at the PCC. The modelling is divided into two,

the first signal modelling is the PWMSTATCOM's dynamic voltage response which is obtained by applying a small (AC) signal on top of the DC operating points called large signal while the second modelling is to obtain DC operating point of PWMSTATCOM at PCC called small signal.

PWMSTATCOM dynamic voltage (large signal). The voltage at the PCC (V_{sa} , V_{sb} and V_{sc}) are being regulated by PWMSTATCOM with (i_{La} , i_{Lb} and i_{Lc}) while (i_a , i_b and i_c) are controlled. The relationship is presented in Eqs. (25)–(30), where (V_{null}) is the voltage of the AC system neutral point with respect to the midpoint of the VSC DC bus. When space phasor of balanced 3-phase is considered, the sinusoidal function is produced in (31), (\hat{f}), (θ_0) and (w) are amplitude, phase angle and angular frequency. The sinusoidal function of the space phasor is given in Eq. (32), Eqs. (25) and (26) are multiplied both sides by the Eq. (32) and added to Eq. (33). Space phasor does not contain (V_{null}), therefore, Eqs. (25)–(27) are added to produce Eq. (34).

$$V_{sa} = L_g \frac{di_{ga}}{dt} + V_{ga} + V_{null}, \tag{25}$$

$$V_{sb} = L_g \frac{di_{gb}}{dt} + V_{gb} + V_{null}, \tag{26}$$

$$V_{sc} = L_g \frac{di_{gc}}{dt} + V_{gc} + V_{null}, \tag{27}$$

$$i_{ga} = i_a - i_{La}, \tag{28}$$

$$i_{gb} = i_b - i_{Lb}, \tag{29}$$

$$i_{gc} = i_c - i_{Lc}, \tag{30}$$

$$f_{a(t)} = \hat{f} \cos(wt + \theta_0), f_{b(t)} = \hat{f} \cos\left(wt + \theta_0 - \frac{2\pi}{3}\right),$$

$$f_{c(t)} = \hat{f} \cos\left(wt + \theta_0 - \frac{4\pi}{3}\right), \tag{31}$$

$$\vec{f}(t) = \frac{2}{3} \left(e^{j0} f_{a(t)} + e^{j\frac{2\pi}{3}} f_{b(t)} + e^{j\frac{4\pi}{3}} f_{c(t)} \right), \tag{32}$$

$$\vec{V}_s = L_g \frac{d\vec{i}_g}{dt} + \vec{V}_g, \tag{33}$$

$$\vec{i}_g = \vec{i} - \vec{i}_L. \tag{34}$$

Consider the AC voltage (V_{ga} , V_{gb} , and V_{gc}) :

$$V_{ga} = \hat{V}_g \cos(w_0t + \theta_0), V_{gb} = \hat{V}_g \cos\left(w_0t + \theta_0 - \frac{2\pi}{3}\right),$$

$$V_{gc} = \hat{V}_g \cos\left(w_0t + \theta_0 - \frac{4\pi}{3}\right). \tag{35}$$

When Eq. (35) is multiplied by Eq. (32), Eq. (36) is obtained. From Fig. 6, If (dq) frame with angle (p) is used to control PWMSTATCOM, Eq. (17) can be substituted for to give Eq. (37) similarly, Eq. (32) is substituted to give (35). Following the similar substitution in Eq. (34), Eqs. (39) and (40) are obtained. By comparison, the real and imaginary component can be obtained through derivative of Eq. (36) multiply by e^{jp} to obtain Eqs. (41) and (42). Where ($w = \frac{dp}{dt}$) and (w) is controlled by a phase lock loop (PLL) based on Eq. (43). The [$w(t)$] in Eq. (43) represents a nonzero steady state value when (V_{sd}) settle at zero. Dynamic system is represented by Eqs. (39)–(43), where (V_{sq}) is the output, (I_d) and (I_q) are controlled input (I_{Id}) and (I_{Iq}) are disturbance inputs. Hence, the dynamic variable is (w) depends on the operating point, but to further clarify the operating point, (V_{sq}) is substituted for in Eqs. (39) and (40) respectively. The dynamic responses of (p) and (w) are indicated in Eq. (44) where their natural and forced transient components are equal to zero.

$$\vec{V}_g = \hat{V}_g e^{j(w_0t + \theta_0)}, \tag{36}$$

$$\vec{V}_s = V_{sdq} e^{jpt}, \vec{i}_g = i_{gdq} e^{jpt}, \vec{V}_g = \hat{V}_g e^{j(w_0 t + \theta_0)},$$

$$V_{sdq} e^{jpt} = L_g \frac{d}{dt} (i_{gdq} e^{jpt}) + \hat{V}_g e^{j(w_0 t + \theta_0)}, \tag{37}$$

$$\vec{i}_g = i_{gdq} e^{jpt}, \vec{i} = i_{dq} e^{jpt}, \vec{i}_L = i_{Ldq} e^{jpt},$$

$$i_{gdq} = i_{dq} - i_{Ldq}, \tag{38}$$

$$i_{gd} = i_d - i_{Ld}, \tag{39}$$

$$i_{gq} = i_q - i_{Lq}, \tag{40}$$

$$V_{sd} = L_g \frac{di_{gd}}{dt} - L_g w_0 i_{gq} + \hat{V}_g \cos(w_0 t + \theta_0 - p), \tag{41}$$

$$V_{sq} = L_g \frac{di_{gq}}{dt} - L_g w_0 i_{gd} + \hat{V}_g \sin(w_0 t + \theta_0 - p), \tag{42}$$

$$\frac{dp}{dt} = w(t) = H(p) V_{sq}^{(t)}, \tag{43}$$

$$\frac{dp}{dt} = L_g H(p) \left(\frac{di_{gq}}{dt} + w_0 i_{gd} \right) + \hat{V}_g H(p) \sin(w_0 t + \theta_0 - p). \tag{44}$$

PWMDSTATCOM dynamic voltage (small signal). The dynamic voltage at PCC (small signal) can be obtained from the Eqs. (41)–(43) around a steady state operating point. Let perturbed variable be defined below, if $\tilde{p}/p_0 \ll 1$, then Eq. (46) is obtained. From (46), perturbed variable is substituted equations in (48)–(50). Substitute for $\hat{V}_g \cos p_0$ and $\hat{V}_g \sin p_0$ in Eqs. (49) and (50) from (47) and (48). Similarly, perturbed (45) is substituted for in Eqs. (43) and (44) and Eq. (50) is deduced. The Laplace transform of the Eqs. (49)–(51) produced Eqs. (52) and (53). The Eqs. (49)–(51) and its Laplace transforms (52)–(54) described a linear system that is the small signal equivalent of the system as described by the Eqs. (41)–(43). The dynamics of $\hat{V}_{sd}(s)$ in terms of $\hat{I}_{gd}(s)$ and $\hat{I}_{gq}(s)$ can be obtained by elimination of $\hat{V}_{sq}(s)$ in (38) and (39), then \tilde{p} can be substituted in (37) thus, (40) is obtained. Where $G_d(s)$ and $G_q(s)$ are transfer function, which has parameters of I_{gd0} and I_{gq0} . $I_d = 0$, $I_{d0} = \hat{I}_d = 0$, then the STATCOM exchange a small amount of real power with PCC, such that $P_s = 0$ and the DC side power of $P_{loss} = VDC_{loss}$. Based on the Eqs. (39) and (40), Eqs. (56)–(59) are obtained. When \hat{I}_{gd} and \hat{I}_{gq} from the Eqs. (58) and (59) are substituted for in Eq. (55), the load and control effects are obtained in Eq. (60).

$$V_{sd} = V_{sd0} + \tilde{V}_{sd},$$

$$V_{sq} = 0 + \tilde{V}_{sq},$$

$$i_{gd} = i_{gd0} + \tilde{i}_{gd},$$

$$w_0 t + \theta_0 - p = -(p_0 + \tilde{p}) \Rightarrow \underbrace{\frac{dp}{dt}}_w = w_0 + \underbrace{\frac{d\tilde{p}}{dt}}_w, \tag{45}$$

$$\cos(p_0 + \tilde{p}) \approx \cos p_0 - (\sin p_0) \tilde{p},$$

$$\sin(p_0 + \tilde{p}) \approx \sin p_0 + (\cos p_0) \tilde{p}, \tag{46}$$

$$V_{sd0} = -L_g w_0 i_{gd0} + \hat{V}_g \cos p_0, \tag{47}$$

$$0 = L_g w_0 i_{gd0} - \hat{V}_g \sin p_0, \tag{48}$$

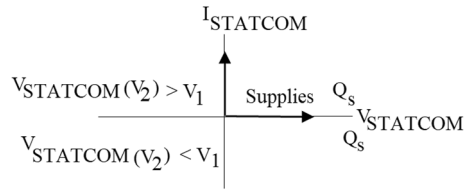


Figure 10. PWMSTATCOM power operation.

$$\tilde{V}_{sd} = L_g \frac{d\tilde{i}_{gd}}{dt} - L_g^{woi_{gd}} - L_g^{i_{gd0}\tilde{w}} - (\tilde{V}_g \sin p_0)\tilde{p}, \tag{49}$$

$$\tilde{V}_{sq} = L_g \frac{d\tilde{i}_{gq}}{dt} - L_g^{woi_{gq}} - L_g^{i_{gq0}\tilde{w}} - (\tilde{V}_g \cos p_0)\tilde{p}, \tag{50}$$

$$\frac{d\tilde{p}}{dt} = \tilde{w} = H(p)\tilde{V}_{sq}, \tag{51}$$

$$\tilde{V}_{sd^{(s)}} = L_g^{s\tilde{i}_{gd^{(s)}}} - L_g^{wo\tilde{i}_{gd^{(s)}}} - L_g(i_{gd0^s} + wo\tilde{i}_{gd0})\tilde{p}^{(s)}, \tag{52}$$

$$\tilde{V}_{sq^{(s)}} = L_g^{s\tilde{i}_{gq^{(s)}}} + L_g^{wo\tilde{i}_{gq^{(s)}}} + L_g(i_{gq0^s} + wo\tilde{i}_{gq0})\tilde{p}^{(s)}, \tag{53}$$

$$\tilde{p}^{(s)} = \frac{H(s)}{s}\tilde{V}_{sq^{(s)}}, \tag{54}$$

$$\tilde{V}_{sd^{(s)}} = G_{d^{(s)}}\tilde{i}_{gd^{(s)}} + G_{q^{(s)}}\tilde{i}_{gd^{(s)}}, \tag{55}$$

$$i_{gd0} \approx -i_{Ld0}, \tag{56}$$

$$i_{gq0} = i_{q0} - i_{Lq0}, \tag{57}$$

$$\tilde{i}_{gd} \approx -\tilde{i}_{Ld}, \tag{58}$$

$$\tilde{i}_{gq} = \tilde{i}_q - \tilde{i}_{Lq}, \tag{59}$$

$$\tilde{V}_{sd^{(s)}} = \underbrace{-G_{d^{(s)}}\tilde{i}_{Ld^{(s)}} - G_{q^{(s)}}\tilde{i}_{Lq^{(s)}}}_{load\ effect} + \underbrace{-G_{q^{(s)}}\tilde{i}_q^{(s)}}_{load\ effect}. \tag{60}$$

Regulatory capability of PWMSTATCOM. The PWMSTATCOM regulation operation and the control diagram are depicted in Figs. 10 and 11⁶¹, where (V2) is the PWMSTATCOM voltage and (V1) is the PCC voltage. If the voltage (V2) is lower than (V1), the current in the inductor is slightly displaced from the voltage (V1) produces an inductive current, then (Qs) becomes positive and PWMSTATCOM absorbs reactive. When the voltage of the PWMSTATCOM exceeds the PCC voltage, the current across the inductor is slightly offset from the voltage V1 that provides a capacitive current, then (Qs) is negative and the PWMSTATCOM produces a reactive power. When the voltage of the PWMSTATCOM is equal to the voltage of the PCC the current through the inductor is nil and consequently there is no power exchange⁶².

The 3-three voltage (V1) is matched by Phase Locked Loop (PLL), the direct axis and quadrature axis mechanisms of 3-three alternating current such as (V_d, V_q, I_d and I_q) are configured by the output of the PLL (angle θ = ωt). The measured (d) and (q) mechanisms of (AC) positive sequence voltage/current, composed with (DC) voltage (V_{dc}) are controlled. An outer regulation loop comprises of an AC voltage regulator and a DC voltage regulator. The reference current (I_{qref}) for the current regulator is from the output of AC voltage regulator (I_q = current in quadrature with a voltage that controls reactive power flow). The reference current (I_{dref}) for the current regulator is from the output of the DC voltage regulator (I_d = current in phase with voltage that controls the active power flow). An inner current control-loop system consisting of a current regulator/or controller, which control the direct current (I_d), the quadrature current (I_q), and the active and reactive power. The magnitude and phase

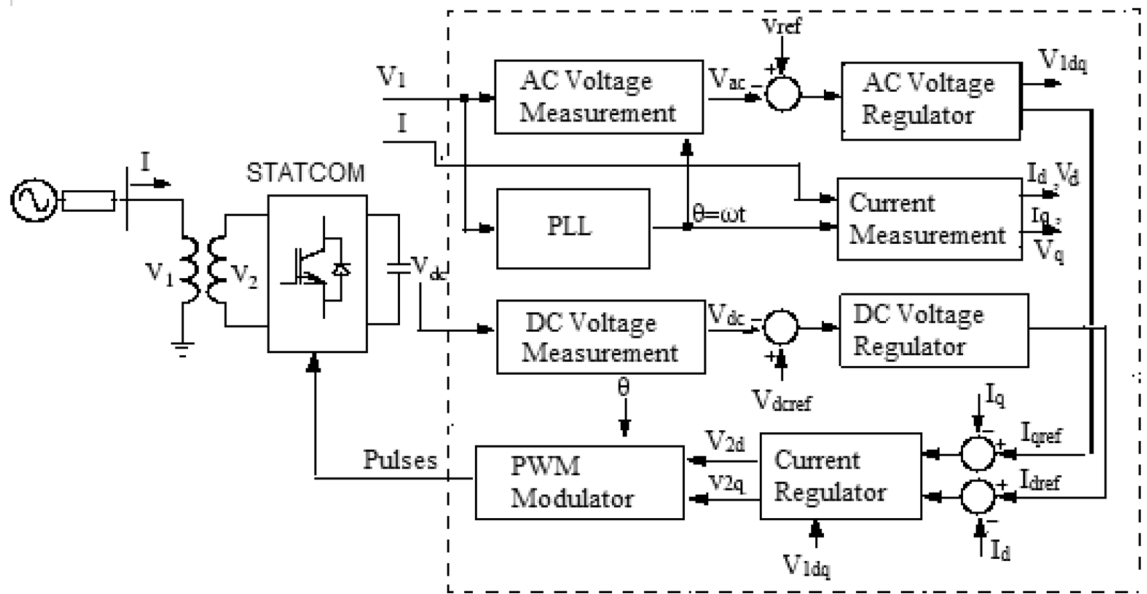


Figure 11. PWMSTATICOM and its control system.

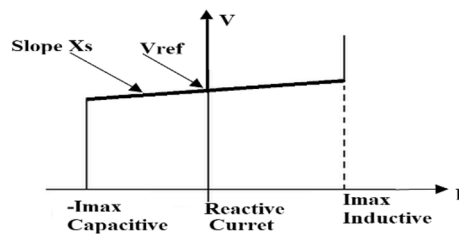


Figure 12. Voltage/current feature.

of the voltage generated by the PWMSTATICOM converter (V_{2d} V_{2q}) from the (I_{dref}) are being controlled by current regulator, while DC voltage regulator and the AC voltage regulator (in voltage control mode) produces (I_{qref}) reference currents. The direct power type regulator that predicts the voltage output, V_2 (V_{2d} V_{2q}) from measurement V_1 (V_{1d} V_{1q}) and the leakage reactivity of the transformer assist the current regulator. The change in reactive power is achieved by means of a voltage source converter connected to the secondary side of a coupler transformer. The voltage source converter utilizes forced-commutated power electronic devices (GTOs, IGBTs or IGCTs) to create a voltage (V_2) from a DC voltage source. There are two ways in which PWMSTATICOM can be used, VAR control and voltage regulation mode. When PWMSTATICOM is in VAR control mode, its reactive power is maintained constant. In the voltage regulation mode, if the reactive current remains within the minimum current values ($-I_{max}$, I_{max}) imposed by the nominal value of the converter, the voltage is controlled to the reference voltage V_{ref} . However, a voltage droop is usually used between 1 and 4% at maximum reactive power output and the V–I characteristic has the slope indicated in Fig. 12⁶³ the V–I characteristic is stated in equation⁶⁰. Inductive current is generated when current (I) is greater zero, while capacitive current is produced when the current generate is less than zero and reactive current when the current is zero as shown in Fig. 12.

$$V = V_{ref} + X_s I. \tag{61}$$

By the adjustment of the phase angle and that of reference point, the bus voltage can be varied with the PWMSTATICOM connected in parallel. When the grid voltage is on the high side or at the lower value over the boundary, PWMSTATICOM behaves in its constant current features. It can produce reactive capacity at the boundary such as capacitive and inductive compensation and independently control its output current over the rated maximum capacitive or inductive range of the amount of AC system voltage.

PCC voltage rise regulation. By considering the electrical distribution network—with a large RDG penetration via PCC. In the case where the power penetration of RDG is 80% of its nominal power rating, there would be the occurrence of voltage rise at PCC. This must be regulated for the continuous operation of RDG as specified by IEEE 1457–2018 and South Africa grid codes. Otherwise, the RDG should be disconnected as per the IEEE 1457–2014 grid code. When the RDG is operating at 90% of its rated nominal power and injected to

Bus 684, the results observed are shown in Fig. 13a–c. Voltage rise occurs up to 1.13 pu as depicted in Fig. 13a without PWMSTATCOM connection to the system, which is not acceptable, the maximum permissible voltage at PCC is 1.1 pu as specified by the South Africa PCC voltage with RDGs integration. The operation of the PWMSTATCOM is shown in Fig. 13b,c, during the voltage rise condition, the operating mode of the PWMSTATCOM changes from the unity power factor to a voltage regulation mode to mitigate the voltage rise at the PCC to an acceptable range in relation to IEEE 1547 and South Africa grid code requirement. It is observed during the voltage regulation mode that the PWMSTATCOM generates reactive power from -0.3 kVAR to -0.02 for the duration of 0.4 s to keep the PCC voltage to 1.1 pu and from -0.02 kVAR to 0.2 kVAR at the duration of 0.4 s to 0.8 s as shown in Fig. 13b, more reactive power is being generated to the PCC by the PWMSTATCOM, the less the occurrence of voltage rise and finally PCC voltage is sustained at 1.09 pu as shown in Fig. 13c between 0.4 and 0.8 s. Hence, the PCC voltage is within an acceptable range in agreement with IEEE 1547 and Southern Africa grid code requirement. The network takes a more RDG penetration level up to 120% with voltage regulation at PCC without violating the grid code act unlike when grid code is violated at 80% penetration without voltage regulation at PCC. Figure 13d–f shows the simulation results when PCC is changed from bus 684 to bus 675 to observe the impact of RDG. Voltage rise occurs between 0.2 and 0.4 s up to 1.15 pu with 85% RDG penetration levels as shown in Fig. 13d, but reactive power is generated by the PWMSTATCOM to the PCC to keep the voltage within an acceptable level as shown in Fig. 13e. The PWMSTATCOM maintains the PCC voltage at 1.1 pu as shown in Fig. 13f while 130% penetration levels are achieved without grid code violation unlike the occurrence of voltage rise at 85% penetration level without PCC regulation. The voltage that flows across the grid is 1.021 pu as shown in Fig. 13g which is within an acceptable range.

Conclusion

The mathematical model of an electrical distribution network with an RDG—penetration has been developed in the paper. The developed model has further been used to investigate the effect of voltage rise and reverse power flow on an electrical distribution network. An advance controller with PWM control-algorithm has also been used to normalize the voltage rise at PCC and to mitigate the reverse power flow problem when operating at a worst critical scenario of minimum load and maximum power output from RDG. Initially, the simulations carried out in the paper has shown that the integration of RDG into a distribution network improve the voltage profile of the power system. However, when a large RDG is considered for integration, there would be a potential voltage rise threat at the PCC. For this scenario, the utility or independent power producers should consider installing an advanced controller at PCC, e.g., the PWM based DSTATCOM, for voltage rise regulation. To further improve the power quality of a large RDG integration at PCC, as a future research direction, online communication model for monitoring of voltage rise when it is out of limit can be considered for continuous measurement of voltages, currents and phase shifts using voltage quality analyzers. An automation system with voltage sensor can be developed, such that it depends on the generation from the RDG facility and the grid voltage for imbalance of electrical consumers at different phases.

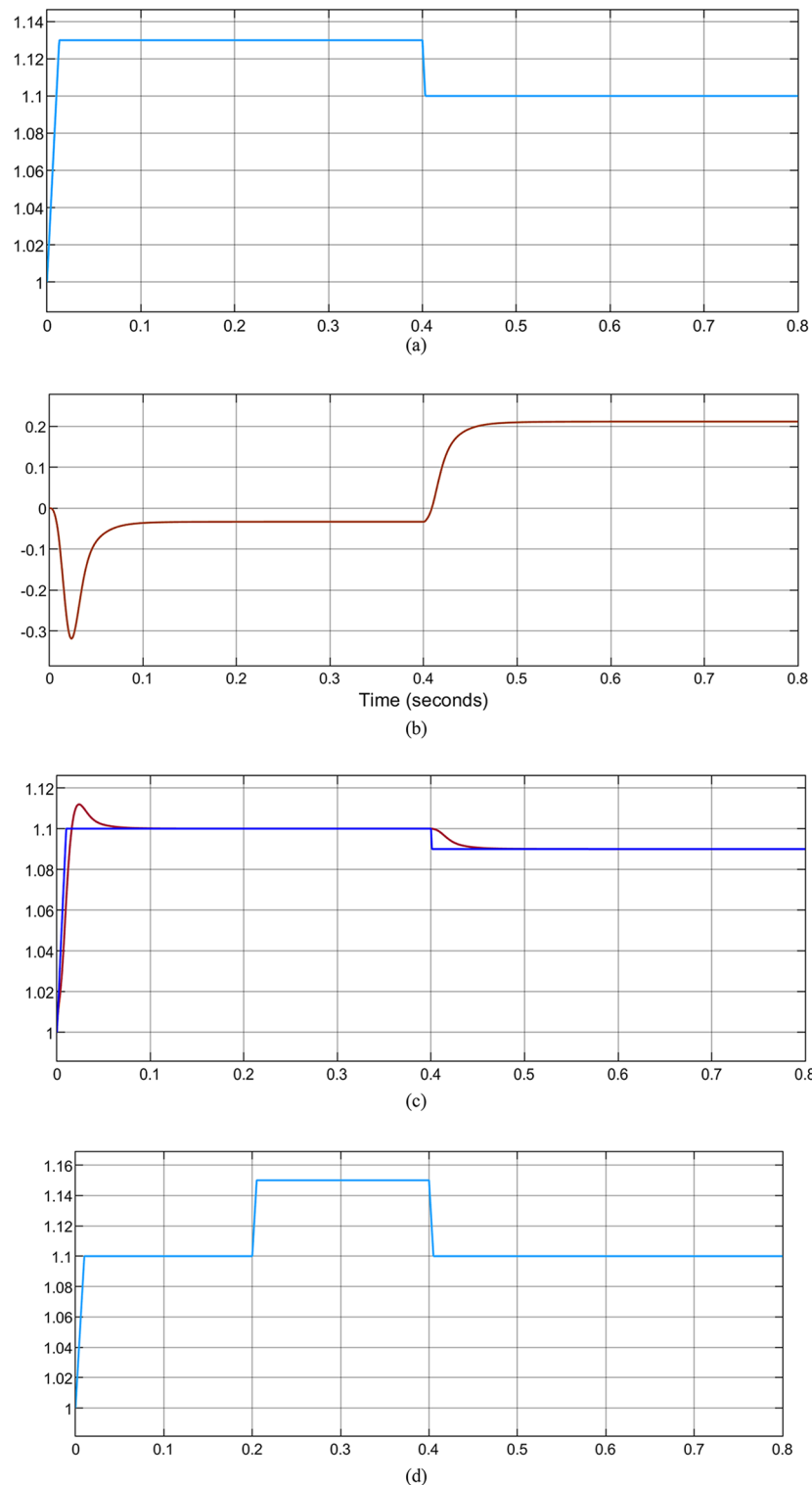


Figure 13. (a) Voltage rise at bus 684 with 80% RDG penetration, (b) reactive power generated by PWMSTATCOM to minimize the voltage rise at PCC, (c) voltage rise regulation at PCC with PWMSTATCOM, (d) voltage rise at bus 675 with 85% RDG penetration, (e) reactive power generated by PWMSTATCOM to regulate voltage rise at PCC, (f) voltage regulation at PCC with PWMSTATCOM and (g) grid voltage during PCC regulation.

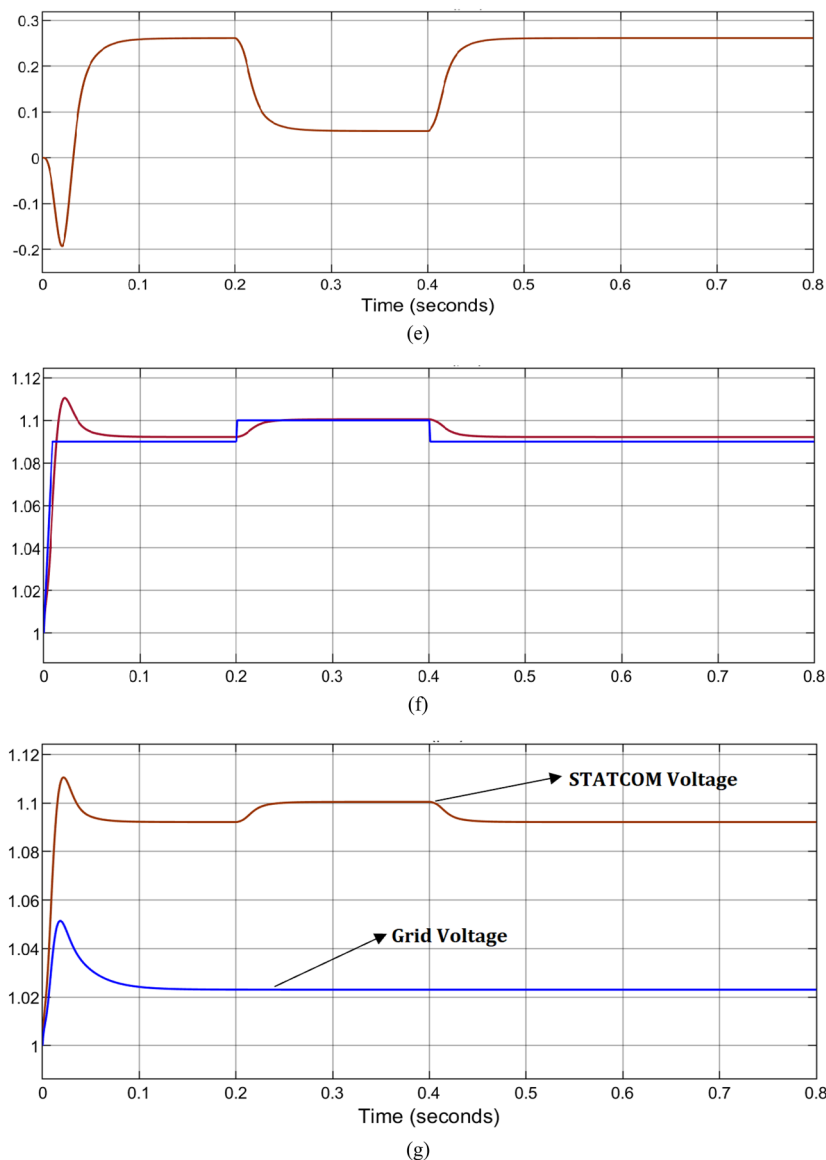


Figure 13. (continued)

Appendix 1

Bus A	Bus B	Active power (KW)	Reactive power (kVAr)	Line length /km	Resistance and reactance/km
632	645	0	0	0	0.625 + j0.3125
632	633	35	6	2	0.625 + j0.3125
633	634	35	6	2	0.625 + j0.3125
645	646	35	6	2	0.625 + j0.3125
650	632	35	6	2	0.625 + j0.3125
684	652	35	6	2	0.625 + j0.3125
632	671	35	6	2	0.625 + j0.3125
671	684	35	6	2	0.625 + j0.3125
671	680	35	6	2	0.625 + j0.3125
671	692	35	6	2	0.625 + j0.3125
684	611	35	6	2	0.625 + j0.3125
692	675	50	20	5	0.625 + j0.3125

Received: 29 December 2021; Accepted: 27 April 2022

Published online: 12 May 2022

References

- Khan, M. N. *et al.* Transformer less inverter topologies for single-phase photo-voltaic systems: A comparative review. *IEEE J. Emerg. Sel. Top. Power Electron.* **8**(1), 805–835 (2020).
- Reshikeshan, S. M., Matthiesen, S. L., Illindala, M. S., Renjit, A. A. & Roychowdhury, R. Autonomous voltage regulation by distributed PV inverters with minimal inter-node interference. *IEEE Trans. Ind. Appl.* **57**(3), 2058–2066 (2021).
- Badal, F. R., Das, P., Sarker, S. K. & Das, S. K. A survey on control issues in renewable energy integration and microgrid. *Prot. Control Mod. Power Syst.* **8**(4), 1–27 (2019).
- Memmel, E. *et al.* Forecast of renewable curtailment in distribution grids considering uncertainties. *IEEE Access* **9**, 60828–60840 (2021).
- Jahangiri, P. & Aliprantis, D. C. Distributed volt/var control by PV inverters. *IEEE Trans. Power Syst.* **28**(3), 3429–3439 (2013).
- Turitsyn, K., Sulc, P., Backhaus, S. & Chertkov, M. Options for control of reactive power by distributed photovoltaic generators. *Proc. IEEE* **99**(6), 1063–1073 (2011).
- Kim, Y., Ahn, S., Hwang, P., Pyo, G. & Moon, S. Coordinated control of a DG and voltage control devices using a dynamic programming algorithm. *IEEE Trans. Power Syst.* **28**(1), 42–51 (2013).
- Dowell, J. & Pinson, P. Very short-term probabilistic wind power forecasts by sparse vector auto-regression. *IEEE Trans. Smart Grid* **7**(2), 763–770 (2016).
- Bollen, M. H. & Sannino, A. Voltage control with inverter-based distributed generation. *IEEE Trans.* **20**(1), 519–520 (2005).
- Carvalho, P. M., Correia, P. F. & Ferreira, L. A. Distributed reactive power generation control for voltage rise mitigation in distribution networks. *IEEE Trans. Power Syst.* **23**(2), 766–772 (2008).
- Deshmukh, S., Pahwa, A. & Natarajan, B. Voltage/VAR control in distribution networks via reactive power injection through distributed generators. *IEEE Trans. Smart Grid.* **3**(3), 1226–1234 (2012).
- Sansawatt, T., Ochoa, L. F. & Har, G. P. Smart decentralized control of DG for voltage and thermal constraint management. *IEEE Trans. Power Syst.* **27**(3), 1637–1645 (2012).
- Degefa, M. Z., Lehtonen, M., Millar, R. J., Alahäivälä, A. & Sa, E. Optimal voltage control strategies for day-ahead active distribution network operation. *Electr. Power Syst. Res.* **127**, 41–52 (2015).
- Qiu, H., Gu, W. & You, F. Bilayer distributed optimization for robust microgrid dispatch with coupled individual-collective profits. *IEEE Trans. Sustain. Energy* **12**(3), 1525–1538 (2021).
- Elavarasan, R. M. *et al.* A comprehensive review on renewable energy development, challenges, and policies of leading Indian states with an international perspective. *IEEE Access* **8**, 4432–74457 (2020).
- Gao, H., Chen, J., Diao, J. & Zhang, J. A HEM-based sensitivity analysis method for fast voltage stability assessment in distribution power network. *IEEE Access* **9**, 13344–13353 (2021).
- Xu, S., Xue, Y. & Chang, L. Review of power system support functions for inverter-based distributed energy resources- standards, control algorithms, and trends. *IEEE Open J. Power Electron.* **2**, 644–1314 (2021).
- Wang, P. *et al.* Equivalent model of multi-type distributed generators under faults with fast-iterative calculation method based on improved PSO algorithm. *Prot. Control Mod. Power Syst.* **29**(9), 1–12 (2021).
- Singh, N. K., Elrayyah, A. & Wanik, M.Z. Analysis of voltage rise and optimal PV curtailment strategy for its mitigation. In *IEEE PES Innovative Smart Grid Technologies Europe (ISGT-Europe)*, 610–614 (2020).
- Matkar, G., Dheer, D. K., Vijay, A. S. & Suryanarayana D. A simple mathematical approach to assess the impact of solar PV penetration on voltage profile of distribution network. In *National Power Electronics Conference (NPEC)*, 209–214. (Pune, 2017).
- Dhaval, Y. R. & Saurabh, N. P. Phase shifting strategy for mitigation of local voltage rise in highly PV penetrated distribution network. In *IEEE International Conference on Power Systems (ICPS)*, 1–6 (Kharagpur, 2021).
- Zad, B. B., Lobry, J., Vallée, F. & Durieux, O. Improvement of on-load tap changer performance in voltage regulation of MV distribution. In *International Conference and Exhibition on Electricity Distribution (CIRED)*, 0496 (Stockholm, 2013).
- Keun, S. *et al.* General and simple decision method for DG penetration level in view of voltage regulation at distribution. *Energies* **6**(9), 1–13 (2013).
- Nikolaos, E., Thomas, W., Carlos, G., Tom De, R. & Johan, D. Coordinated voltage control scheme for Flemish LV distribution grids utilizing OLTC transformers and D-STATCOMs. In *IET International Conference on Developments in Power System Protection (DPSP)*, 1–6 (Copenhagen, 2014).
- Luis, R. M. *et al.* Linearly decoupled control of a dynamic voltage restorer without energy storage. *Energies* **8**(10), 1–18 (2020).
- Igor, C. T., Gustavo, F. N. & Chiguero, T. Theoretical and experimental study to determine voltage violation, reverse electric current and losses in prosumers connected to low-voltage power grid. *Energies* **12**(23), 1–20 (2019).
- Edoardo, D., Marco, P., Ferdinanda, P. & Antonello, M. A coordinated voltage control for overvoltage mitigation in LV distribution grids. *Energies* **3**(8), 1–20 (2007).
- Dilini, A., Jagadeesh, P., Shangari, K. R. & Reyasudin, B. K. Performance evaluation of solar PV inverter controls for overvoltage mitigation in MV distribution networks. *Energies* **10**(12), 1–14 (2021).
- Shakir, D. A., Fahad, S. M., Shafiqullah, M., Fahad, A. A. & Ibrahim, M. E. Grid integration challenges of wind energy: A review. *IEEE Access* **8**, 10857–10878 (2020).
- Mahela, O. P., Gupta, N., Khosravy, M. & Patel, N. Comprehensive overview of low voltage ride through methods of grid integrated wind generator. *IEEE Access* **7**, 99299–99326 (2019).
- Vargas, U. & Ramirez, A. Extended harmonic domain model of a wind turbine generator for harmonic transient analysis. *IEEE Trans. Power Deliv.* **31**(3), 1360–1368 (2016).
- Glover, J. D., Sarma, M. S. & Overbye, T. *Power System Analysis & Design, SI Version* (Cengage Learning, 2012).
- El-Sattar, A., Saad, N. & El-Dein, M. S. Dynamic response of doubly fed induction generator variable speed wind turbine under fault. *Electr. Power Syst. Res.* **78**(7), 1240–1246 (2008).
- Zhu, D. *et al.* Inductance emulating control for DFIG-based wind turbine to ride-through grid faults. *IEEE Trans. Power Electron.* **32**(11), 8514–8525 (2017).
- Mohammadi, J., Vaez-Zadeh, S., Afsharnia, S. & Farhangi, S. Improved fault ride through strategy for doubly fed induction generator based wind turbines under both symmetrical and asymmetrical grid faults. *IET Renew. Power Gener.* **10**(8), 1114–1122 (2016).
- Naderi, S. B., Negnevitsky, M., Jalilian, A., Hagh, M. T. & Muttaqi, K. M. Optimum resistive type fault current limiter: An efficient solution to achieve maximum fault ride-through capability of fixed-speed wind turbines during symmetrical and asymmetrical grid faults. *IEEE Trans. Ind. Appl.* **53**(1), 538–548 (2017).
- Worku, M. Y., Abido, M. A. & Iravani, R. PMSG based wind system for real-time maximum power generation and low voltage ride through. *J. Renew. Sustain. Energy* **9**(1), 013304 (2017).
- Amin, J., Kashem, M. M. & Danny, S. A novel voltage clamping-based overvoltage protection strategy to avoid spurious trip of inverter-based resources and eliminate the risk of wildfire following the REFCL operation in compensated networks. *IEEE Trans. Ind. Appl.* **57**(5), 4558–4568 (2021).

39. NERSA. *Grid Connection Code for Renewable Power Plants (RPPs) Connected to the Electricity Transmission System (TS) or the Distribution System (DS) in South Africa* (RSA Grid Code Secretariat, 2014).
40. Kersting, W. H. Radial distribution test feeders. In *Power Engineering Society Winter Meeting*, 2, 908–912 (IEEE Power Engineering Society Winter Meeting, 2001).
41. Kersting, W. H. Radial distribution test feeders. *IEEE Trans. Power Syst.* **6**(3), 975–985 (1991).
42. IEEE Standard. *IEEE Recommended Practice and Requirements for Harmonic Control in Electric Power Systems* (IEEE Standard, 2014).
43. Karmakar, N. & Bhattacharyya, B. Hybrid intelligence approach for multi-load level reactive power planning using VAR compensator in power transmission network. *Prot. Control Mod. Power Syst.* **26**(6), 1–17 (2021).
44. Hu, H. *et al.* Grid impedance impact analysis of the weak grid-tied VSC. In *IEEE Green Technologies Conference (Greentech)* (Denver, 2021).
45. Dugan, R. C., McGranaghan, M. F., Santosa, S. & Beaty, H. W. *Electric Power Systems Quality* (McGraw-Hill, 2002).
46. Blazic, B. & Papic, I. Voltage profile support in distribution networks—Influence of the network R/X ratio. In *International Power Electronics and Motion Control Conference* (Poznan, 2008).
47. Akinyemi, A. S. & Awodele, K. Voltage profiles improvement with wind energy converter connected to a distribution network. *Southern African University Power Engineering Conference (SAUPEC)* (Johannesburg, 2015).
48. Mahdavi, S., Panamtaash, H., Dimitrovski, A. & Zhou, Q. Predictive coordinated and cooperative voltage control for systems with high penetration of PV. *IEEE Trans. Ind. Appl.* **57**(3), 2212–2222 (2021).
49. Sree, L. K., & Vijaya, K. M. Dynamic voltage stability enhancement of a wind farm connected to grid using facts—A comparison. In *International Conference on Circuits and Systems in Digital Enterprise Technology (ICCSDET)*, 1–5 (Kottayam, 2020).
50. Tian, C., Chenghao, L., Gao, Z., Rao, Y., Cui, W. & Xueqing, P. Study on different modes of reactive power compensation and reactive power coordinated control for wind farm. In *IEEE Industrial and Commercial Power System*, 340–345 (2020).
51. Dorile, P. O., Jagessar, D. R., Guardado, L., Jagessar, S. S. & McCann, R. A. Power system stabilization of a grid highly penetrated from a variable-speed wind based farm through robust means of STATCOM and SSSC. In *International Conference on Engineering of Modern Electric Systems (EMES)* (Oradea, 2021).
52. Dash, R. L., Tripathy, S., Mohanty, B. & Hota, P. K. Power quality improvement of grid connected wind system with STATCOM. In *International Conference on Power Electronics and Energy (ICPEE)* (Bhubaneswar, 2021).
53. Arrik, K. & Sirdeep, S. Integration of wind farm in power system using STATCOM. *Int. J. Sci. Eng. Res.* **4**(4), 1293–1299 (2013).
54. Hasan, S. & Agarwal, V. An unconstrained voltage support scheme for distributed generation connected to resistive-inductive grid under unbalanced conditions. *IEEE Trans. Ind. Appl.* **57**(4), 4253–4262 (2021).
55. Canizares, C. Power flow and transient stability models of FACTS controllers for voltage and angle stability studies. *IEEE Power Eng. Soc. Winter Meet.* **2**, 1447–1454 (2000).
56. Alinezhad, M. A. & Kamarposhti, M. Comparison of SVC and STATCOM in static voltage stability margin enhancement. *Int. Sci. Index* **3**(2), 722–727 (2009).
57. Lee, G., Hwang, P. & Moon, S. Reactive power control of hybrid multi-terminal HVDC systems considering the interaction between the AC network and multiple LCCs. *IEEE Trans. Power Syst.* **36**(5), 4562–4574 (2021).
58. Yazdani, A. & Iravani, R. *Voltage Converters in Power System* (Wiley, 2010).
59. Mosaad, M. I., Ramadan, H. S., Aljohani, M., El-Naggar, M. F. & Ghoneim, S. S. Near-optimal PI controllers of STATCOM for efficient hybrid renewable power system. *IEEE Access* **9**, 34119–34130 (2021).
60. Zhou, X. *et al.* Control strategy research of D-STATCOM using active disturbance rejection control based on total disturbance error compensation. *IEEE Access* **9**, 50138–50150 (2021).
61. Oghorada, O. J., Zhang, L., Han, H., Esan, A. B. & Mao, M. Inter-cluster voltage balancing control of a delta connected modular multilevel cascaded converter under unbalanced grid voltage. *Protect. Control Mod. Power Syst.* **23**(6), 1–11 (2021).
62. Ranjan, S. *et al.* Maiden voltage control analysis of hybrid power system with dynamic voltage restorer. *IEEE Access* **9**, 60531–60542 (2021).
63. Woo, J. H., Wu, L., Lee, S. M., Park, J. & Roh, J. H. D-STATCOM d-q axis current reference control applying DDPG algorithm in the distribution system. *IEEE Access* **9**, 145840–214585 (2021).

Author contributions

A.S.A.: Conceptualization; Methodology; Software; Validation. Formal analysis; Investigation, Writing original draft. K.M.: Formal analysis, Writing review; Supervision; Project administration. I.E.D.: Conceptualization, Methodology, Resources; Writing, Editing; Co-supervisor; Funding/APF.

Competing interests

The authors declare no competing interests.

Additional information

Correspondence and requests for materials should be addressed to A.S.A.

Reprints and permissions information is available at www.nature.com/reprints.

Publisher's note Springer Nature remains neutral with regard to jurisdictional claims in published maps and institutional affiliations.



Open Access This article is licensed under a Creative Commons Attribution 4.0 International License, which permits use, sharing, adaptation, distribution and reproduction in any medium or format, as long as you give appropriate credit to the original author(s) and the source, provide a link to the Creative Commons licence, and indicate if changes were made. The images or other third party material in this article are included in the article's Creative Commons licence, unless indicated otherwise in a credit line to the material. If material is not included in the article's Creative Commons licence and your intended use is not permitted by statutory regulation or exceeds the permitted use, you will need to obtain permission directly from the copyright holder. To view a copy of this licence, visit <http://creativecommons.org/licenses/by/4.0/>.

© The Author(s) 2022